GEOPHYSICAL RESEARCH LETTERS, VOL. 16, NO. 8, PAGES 941-944, AUGUST 1989

# STRATOSPHERIC AEROSOLS FROM $CH_4$ PHOTOCHEMISTRY ON NEPTUNE

Paul. N. Romani

Science Systems and Applications, Inc.

Sushil K. Atreya

Department of Atmospheric, Oceanic and Space Sciences,
The University of Michigan

Abstract. We have used a combined photochemical-condensation model to study hydrocarbon ices produced from $CH_4$ photolysis in the stratosphere of Neptune. We predict a total stratospheric haze production rate of $4.2 \times 10^{-15}$ grams $cm^{-2}$ $s^{-1}$ (75% ethane, 25% acetylene, trace diacetylene). The total production rate is insensitive to within a factor of two to order of magnitude changes in the eddy diffusion coefficient and methane mixing ratio, which is within our estimate of uncertainty for this number. The condensation temperatures are 97 K for $C_4H_2$, 71 K for $C_2H_2$, and 64 K for $C_2H_6$. Voyager 2 images of Neptune will be able to confirm the presence of stratospheric aerosols and provide constraints on their production rate and location.

## Introduction

Analysis of high phase angle Voyager 2 images of Uranus done in Pollack et al. [1987] showed first, the presence of stratospheric hazes and second, combined with a cloud microphysics model placed constraints on the production rate and location of the aerosols. On the eve of Voyager 2's encounter with Neptune we present our latest modelling predictions about the production rates, location, and composition of hazes from methane photochemistry in the stratosphere of Neptune.

There is evidence for stratospheric aerosols on Neptune from ground based observations in the near IR. The 0.9μm methane band of Neptune has a residual intensity of 1%. In the absence of any stratospheric aerosols it would have a residual intensity of only 0.1% [Bergstralh et al., 1987]. Bergstralh et al. deduce an optical depth of 0.1 to 0.25 at 0.9μm depending on the pressure level of the hazes (0.001-0.02 bar). Recently Hammel [1988] from an analysis of the center-to-limb profile of this methane band deduced the presence of some scattering material above the 0.005 bar level.

The likely source of these aerosols are hydrocarbons produced by the photolysis of methane. We have shown previously that photochemical production of ethane, acetylene, and diacetylene from methane photolysis will lead to production of their respective hydrocarbon ice hazes in the 0.002-0.01 bar region [Romani and Atreya, 1988]. The other possible source of stratospheric aerosols is methane ice crystals being transported from the methane ice cloud formation region in the troposphere (≈ 1.5 bar level) into the stratosphere. Presently it is believed that sublimating $CH_4$ ice crystals are the source of the observed supersaturation of methane above the cold trap on Neptune, 2% vapor phase mixing ratio [Orton et al., 1987]. However, the sublimating methane ice crystals will be in equilibrium with this mixing ratio at ≈64K, (about 0.02 bar level), and we do not expect them to survive to much lower pressures. $PH_3$ and/or $NH_3$ photochemistry which can also produce aerosols [West et al., 1986], will not occur on Neptune because of the removal of the parent species in the lower troposphere by condensation.

Previously in our modelling we had assumed an abrupt conversion of the photochemical profile to a saturation limited one. We now include a loss process due to condensation in the model. This improvement allows for a better calculation of the total haze production rate, the partitioning of the haze production rate among the condensing species, and the effects condensation has upon the mixing ratio profiles of the condensing species.



Paper number 89GL00936.
0094-8276/89/89GL-00936$03.00

## Numerical Model

### Photochemical

The photochemical part of this model used in this study has been described previously [Romani and Atreya, 1988]. The major change since then is the inclusion of $C_4H_2$ chemistry into the model; no longer is it solved for separately. Acetylene is the parent molecule for diacetylene, but diacetylene undergoes recycling to acetylene. Including both species in the photochemical model allows for feedback to occur between the two. The model is one dimensional and solves the coupled continuity equations for methane and its photolysis products by using an iterative Newton-Raphson technique. Eddy mixing is parameterized by the use of an eddy diffusion coefficient, K. The molecular diffusion coefficients for the chemical species are the same as before with the exception of $C_4H_2$ which is estimated using techniques given in Reid et al. [1977]. Methane ($CH_4$), methyl radical ($CH_3$), ethylene ($C_2H_4$), acetylene ($C_2H_2$), ethane ($C_2H_6$), diacetylene ($C_4H_2$) and atomic hydrogen (H), undergo eddy and molecular diffusion and photochemical reactions. The radicals; CH, $^3CH_2$, $^1CH_2$, $C_2H$, $C_2H_3$, $C_2H_5$, $C_4H$, and $C_4H_3$ are assumed to be in photochemical equilibrium. From comparison of model results to observations of the hydrocarbons in the stratospheres of Jupiter, Saturn, and Uranus, we estimate an uncertainty of a factor of two in the predicted mixing ratios.

Fixed-point boundary conditions and a convergence criteria of 1% was used for all studies. Changes in the lower boundary values of $C_4H_2$, $C_2H_2$, and $C_2H_6$ by an order of magnitude did not propagate more than 2 levels above the lower boundary. The upper boundary values for the hydrocarbons were adjusted so there was zero net flux at the upper boundary (placed within an atmospheric scale height above the homopause), while the upper boundary value for atomic hydrogen was adjusted so there was a net downward flux of $4 \times 10^7$ molecules $cm^{-2}$ $s^{-1}$. The H production by solar EUV (photons and photoelectrons) at Jupiter corresponding to the time of the Voyager encounters in 1979 was $1.3 \times 10^9$ $cm^{-2}$ $s^{-1}$. Scaling this to Neptune would give a production rate of $3.5 \times 10^7$. The EUV flux at the time of the Neptune encounter is expected to be greater than that in 1979, as it is already at that level now. So we adjusted this number slightly upward.

Condensation Loss

The loss process of the condensing hydrocarbons; $C_4H_2$, $C_2H_2$, and $C_2H_6$ from is modelled by the diffusive growth rate for ice crystals - vapor phase molecules strike an ice crystal and stick to it. The diffusive mass growth rate (gm $s^{-1}$) per crystal is taken from Pruppacher and Klett [1980];

$$\frac{dm}{dt} = \frac{4 \pi C S Vp D' M}{RT} \qquad (1)$$

Where C is a proportional to the crystal size and a function of the crystal geometry, S the supersaturation, T the absolute temperature, R the universal gas constant, Vp and M are respectively the vapor pressure and the molecular weight of the condensing species, and D' is the molecular diffusion coefficient of the condensing species corrected for gas kinetic effects for small crystals;

$$D' = \frac{D}{\frac{C}{C+\delta} + \frac{D}{C\alpha}\left\{\frac{2\pi M}{RT}\right\}^{1/2}} \qquad (2)$$

$\delta$ is the "thermal jump distance" which is taken to be the mean free path of the atmospheric molecules, a the sticking efficiency, and D the standard molecular diffusion coefficient. In our models we assumed a sticking efficiency of unity. For small crystals the second term in the denominator of (2) dominates and the crystal grows proportional to $C^2$; for large crystals the first term dominates and D' approaches the limit of D and the crystal grows as only C. For consistency with our other calculations we assumed the crystals to be spherical, in which case C equals the radius. For crystals of approximately equal size the variability of C is within a factor of 3. The total ice haze production rate is controlled by the photochemical destruction of methane and the condensation loss rate adjusts the supersaturation to match this. So this variability of C introduces a variability in the supersaturations. Similarly, if we had reduced the sticking efficiency there would have been a corresponding increase in the supersaturation. To determine the supersaturations we used the same vapor pressures as before [Romani and Atreya, 1988] with the exception of $C_4H_2$ where we have used the new laboratory data of Hudson et al. [1988];

$$\log_{10}(Vp) = 9.582 - \frac{2023.8}{T} \qquad (3)$$

where Vp is the vapor pressure of $C_4H_2$ in mm Hg, and T is the temperature in degrees Kelvin. We are still forced to extrapolate the vapor pressure for $C_4H_2$ over 30°K. The likely bias in doing so is to predict vapor pressures too large and thus a condensation level that is higher in temperature than actual.

Since the above vapor phase loss process is per crystal, a number density profile of the hydrocarbon ice crystals is required. We assumed that all downward transport of the hydrocarbons through the cold trap is by ice crystal sedimentation. At equilibrium, the photochemical column production rate of each species is balanced by the column density of aerosols times an inverse-lifetime. For lifetimes we used the time it takes for the aerosols to fall from the condensation levels to the tropopause (0.1 bar level). For the sizes of particles in our analysis (0.1, 0.2, 0.5, and 1.0 μm radii) the fall velocities were calculated by multiplying their respective Stokes velocities by the Cunningham correction factor. This size range of particles corresponds to the range of particles observed for stratospheric hazes on Jupiter, Saturn, and Uranus [West et al., 1986, Tomasko et al., 1984, Pollack et al. 1987].

First the model was run without condensation and the condensation levels were determined to be where the equilibrium saturation abundances fell below the respective photochemical ones. The resultant column densities were then used as input into the model, but now with the condensation loss turned on. The new condensation levels and photochemical production rates were used to calculate new column densities which were then fed back into the model. This was repeated until convergence occurred. For simplicity we assumed that each species condenses only on its own ice particle. We also assumed then ice crystals were distributed uniformly in height from the respective condensation level to the tropopause.

## Discussion

Mixing Ratio Profiles of $C_4H_2$, $C_2H_2$, and $C_2H_6$

In Figures 1 - 3 we compare the mixing ratio profiles of $C_4H_2$, $C_2H_2$, and $C_2H_6$ from the combined photochemical-condensation model to their respective saturation limited profiles. The relevant model parameters for this standard model (for the purpose of this discussion) are as follows; an eddy diffusion coefficient of $10^6$ $cm^{-2}$ $s^{-1}$ at the methane homopause and inversely proportional to the atmospheric number density, same model atmosphere as Romani and Atreya [1988], solar maximum fluxes (present at the time of the Voyager 2 encounter), diurnally averaged solar fluxes and a solar zenith angle of 50° (global average conditions) and a methane mixing ratio of 2% at the lower boundary. The condensation levels are as follows; $C_4H_2$, 97K and 0.005 bar, $C_2H_2$, 71K and 0.017 bar, and $C_2H_6$, 64K and 0.027 bar. Since $C_2H_2$ and $C_2H_6$ are controlled by eddy diffusion the effects of the condensation sink propagate several scale heights above the condensation level. Diacetylene is close to photochemical equilibrium so its profile shows the sharpest turn over from a photochemical profile to a saturation limited one.

Diacetylene, unlike acetylene or ethane, is supersaturated in its condensation region. $C_2H_2$ and $C_2H_6$ are produced above their condensation region and are transported by eddy diffusion into it. While some of this occurs for $C_4H_2$, most of its haze production is in situ production with chemical

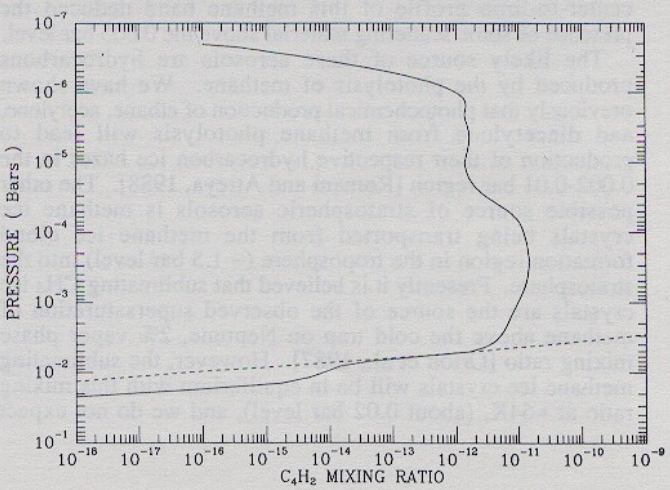


Fig. 1. Diacetylene mixing ratio vs. pressure on Neptune. The dashed line is the mixing ratio from saturation equilibrium over the ice and the solid line is from the combined photochemical-condensation model. See text for model atmosphere assumptions.

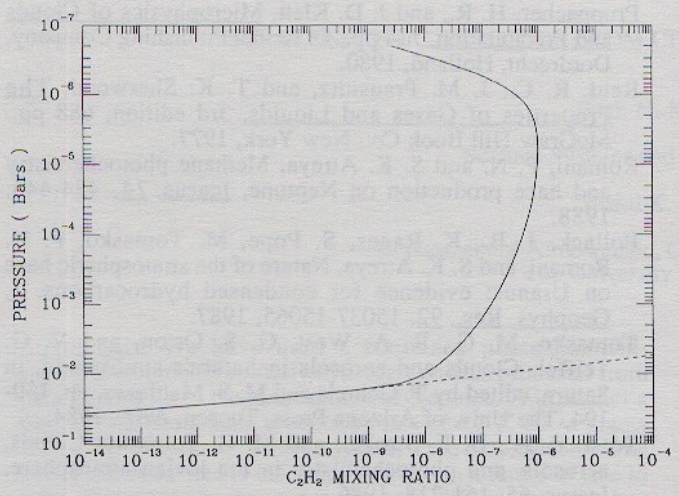


Fig. 2. Same as figure 1 except for Acetylene.

production balanced by condensation loss. Throughout this haze formation region the production rate is relatively constant, but the temperature and, thus, the vapor pressure is dropping exponentially. As can be seen in Eqn. (1) for the condensation loss to balance a constant photochemical production requires the supersaturation to increase as the vapor pressure drops. $C_4H_2$ production ceases below the level of $C_2H_2$ condensation, and we do not have confidence in the predicted $C_4H_2$ mixing ratio there. Supersaturations could also develop for $C_2H_2$ and $C_2H_6$ if there were insufficient numbers of ice crystals on which they could condense. For the column densities we calculated, balancing photochemical production by sedimentation, this never occurred.

The magnitude of the eddy diffusion coefficient in the lower stratosphere controls how much the condensation of $C_2H_2$ and $C_2H_6$ affects their mixing ratio profiles above their condensation levels. To illustrate this, in Figure 3 we show the changes in the $C_2H_6$ profile caused by lowering the eddy diffusion coefficient from $10^6$ to $10^5$ cm$^{-2}$ s$^{-1}$ at the methane homopause but with the same variation in number density. Lowering the eddy diffusion coefficient lowers the ethane production by only 7%. As the eddy diffusion coefficient is lowered the gradient in mixing ratio must increase, since the photochemical production is balanced by eddy transport into the condensation region. This results in a more abrupt cross over from the photochemical to saturation profile. We presently favor a K in the range of $10^5$ to $10^6$ cm$^{-2}$ s$^{-1}$ based on comparison of model output to IR heteroydyne observations of $C_2H_6$ on Neptune (Kostiuk, pers. comm.). The Voyager 2 Ultraviolet Spectrometer will be able to detect the level to which the hydrocarbons are mixed and directly constrain the magnitude of eddy diffusion in the stratosphere of Neptune.

The $C_2H_6$ and $C_2H_2$ mixing ratio profiles are not sensitive to the choice of the methane mixing ratio at the lower boundary. Orton et al. [1987] estimate a 2% stratospheric mixing of $CH_4$ which we adopted here. But if they use their "warm" thermal profile the $CH_4$ mixing ratio would drop to 0.2%. Using the lower amount of methane reduces the mixing ratios by a factor of 1.5.

Haze Production and Variability

The total haze production rate in the standard model is 4.2 X $10^{-15}$ grams cm$^{-2}$ s$^{-1}$, of which 75% is ethane, 25% acetylene, and only a trace diacetylene. This is controlled by the photochemistry, i.e., the conversion rate of $CH_4$ to $C_4H_2$, $C_2H_2$ and $C_2H_6$. Since for even a saturation limited abundance of $CH_4$ there is enough methane to produce a t of 1 in the UV, haze production is primarily a photon limited process. However, the location of the t = 1 level does affect the chemistry that occurs after methane photolysis. If this moves to higher number densities (decreasing the eddy diffusion or the methane mixing ratio at the lower boundary), the conversion of $CH_4$ to higher order hydrocarbons decreases due to changes in which reaction pathways dominate. Nevertheless, the total haze production rate varied by less than a factor of two to the order of magnitude changes in the eddy diffusion coefficient and methane mixing ratio described above.

The composition of this haze also remained unchanged to within a factor of 2 to these changes; the $C_2H_2/C_2H_6$ ratio stayed the same and $C_2H_6$ production was $\approx$ 75% of the total. However, the $C_4H_2$ production rate changed by factors of 3-15, and in the opposite sense as the total haze production rate. Lowering the eddy diffusion coefficient in the lower stratosphere increases the vapor phase $C_2H_2$ mixing ratio and thus increases $C_4H_2$ production; lowering the $CH_4$ mixing ratio lowered the recycling rate of $C_2H_2$ after it underwent photolysis and thus increased $C_4H_2$ production.

The ultimate source for these hazes is the solar UV. Thus the production rate varies with solar activity and the seasonal change in the solar insolation (the cosine of the solar zenith angle times the length of the illuminated day). At the time of the Voyager 2 encounter with Neptune it will be near southern summer solstice; the production rate will be zero in the northern polar night and a maximum in the summer pole (twice the global production rate given here). The $C_4H_2$ haze is produced in situ so it will be directly affected by the variation in solar insulation. However the source for $C_2H_2$ and $C_2H_6$ is above the condensation layer and the relevant time is the transport time from the source region to the condensation region. For our standard case, the eddy transport time in the lower stratosphere is on the order of 0.4 Neptune years, longer than a season and the 11 year solar cycle. Also latitudinal transport of the haze particles themselves can make the hazes more uniform. Here the appropriate time is the particle fall out time. The fall times range from 0.2 Neptune year for 0.1 μm radius particles to 0.01 for 1.0μm.

Thus the hazes will be affected by local dynamics. In particular, the location of the condensation levels is controlled by the temperature since the vapor pressures change by an order of magnitude for a change in temperature of 5K. Any

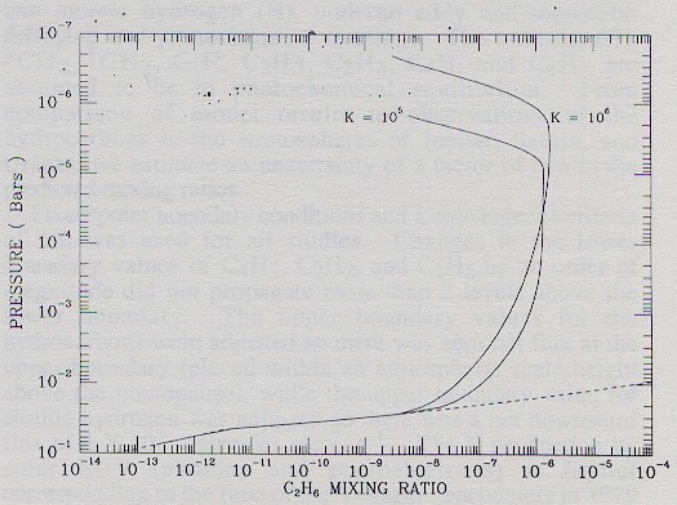


Fig. 3. Ethane mixing ratio vs. pressure on Neptune. The dashed line is the mixing ratio from saturation equilibrium over the ice, the solid curves are from the model with two different values of K at the $CH_4$ homopause, $10^5$ cm$^2$ s$^{-1}$ and $10^6$ cm$^2$ s$^{-1}$ (K proportional to the inverse square root of the atmospheric number density).

process that caused a localized lowering of the temperature would cause haze formation at lower pressures. For observations in methane bands (e.g. Hammel, 1988), this would cause an apparent increase in the optical depth as the scattering now takes place below a lower column abundance of methane.

Acknowledgments. We thank J. Allen, C. Hudson, and R. Khana for assistance in interpreting their $C_4H_2$ vapor pressure data. P. N. Romani acknowledges support at NASA Goddard Space Flight Center, Greenbelt, Maryland, from NASA contract NAS5-3014, S. K. Atreya from NSG-7404, and University of Arizona Voyager Project Number 070485.

## References

Bergstralh, J. T., K. H. Baines, R. J. Terrile, D. Wenkert, J. Neff, and B. A. Smith, Aerosols in the stratosphere of Neptune: constraints from near-IR broadband imagery and UV, blue, and near-IR spectrophotometry (abstract), Bull. Am. Astron. Soc., 19, 639, 1987.

Hammel, H. B., The atmosphere of Neptune studied with CCD imaging at methane-band and continuum wavelengths, Ph D. thesis, 128 pp. The Univ. of Hawaii, May 1988.

Hudson, C. M., J. E. Allen Jr., R. K. Khanna, and G. Kraus, Vapor pressure measurements of hydrocarbons and nitriles (abstract), Bull. Am. Astron. Soc., 20, 857, 1988.

Orton, G. S., D. K. Aitken, C. Smith, P. F. Rouche, J. Caldwell, and R. Snyder, The spectra of Uranus and Neptune at 8-14 and 17-23 μm, Icarus, 70, 1-12, 1987.

Pruppacher, H. R., and J. D. Klett, Microphysics of Clouds and Precipitation, 714 pp., D. Reidel Publishing Company, Dordrecht, Holland, 1980.

Reid, R. C., J. M. Prausnitz, and T. K. Sherwood, The Properties of Gases and Liquids, 3rd edition, 688 pp., McGraw-Hill Book Co., New York, 1977.

Romani, P. N. and S. K. Atreya, Methane photochemistry and haze production on Neptune, Icarus, 74, 424-445, 1988.

Pollack, J. B., K. Rages, S. Pope, M. Tomasko, P. N. Romani, and S. K. Atreya, Nature of the stratospheric haze on Uranus: evidence for condensed hydrocarbons, J. Geophys. Res., 92, 15037-15065, 1987.

Tomasko, M. G., R. A. West, G. S. Orton, and V. G. Teiffel, Clouds and aerosols in Saturn's atmosphere, in Saturn, edited by T. Gehrels and M. S. Matthews, pp. 150-194, The Univ. of Arizona Press, Tucson, Ariz., 1984.

West, R. A., D. F. Strobel, and M. G. Tomasko, Clouds, aerosols, and photochemistry in the jovian atmosphere, Icarus, 65, 161-218, 1986.

Paul N. Romani, Code 693.2, NASA/Goddard Space Flight Center, Greenbelt, MD 20771.

Sushil K. Atreya., Department of Atmospheric, Oceanic and Space Sciences, The University of Michigan, Ann Arbor, MI 48109-2143.

(Received: March 9, 1989;
revised: April 17, 1989;
accepted: April 27, 1989.)